

Binary Homodyne Detection for Observing Quadrature Squeezing in Satellite Links

Christian R. Müller,^{1,2} Kaushik P. Seshadreesan,^{1,2} Christian Peuntinger,^{1,2} and Christoph Marquardt^{1,2}

¹Max Planck Institute for the Science of Light, Staudtstr. 2, 91058 Erlangen, Germany

²Institute of Optics, Information and Photonics, University of Erlangen-Nuremberg, Staudtstr. 7/B2, D-91058 Erlangen, Germany

(Dated: November 26, 2018)

Optical satellite links open up new prospects for realizing quantum physical experiments over unprecedented length scales. We analyze and affirm the feasibility of detecting quantum squeezing in an optical mode with homodyne detection of only one bit resolution, as is found in satellites already in orbit. We show experimentally that, in combination with a coherent displacement, a binary homodyne detector can still detect quantum squeezing efficiently even under high loss. The sample overhead in comparison to non-discretized homodyne detection is merely a factor of 3.3.

PACS numbers: 03.67.Hk, 42.50.Dv, 42.50.Ex

The laws of quantum mechanics have been validated by numerous fundamental tests [1]. With the advent of optical satellite links [2–6] it is now possible to also validate quantum mechanics over vast distances and a varying gravitational potentials. This includes non-classical states [7] such as quadrature squeezed states of the light field [8, 9]. Squeezing is efficiently measured via homodyne detection [10], a measurement technique of utmost importance not only in optics, but in diverse physical architectures such as optomechanical resonators [11], superconducting qubits [12, 13], spin ensembles [14–17] and Bose-Einstein condensates [18]. Homodyne detection yields continuously distributed quadrature projections, which in practice are sometimes deliberately discretized. In optical quantum information processing [19–23] this is exemplified by quantum key distribution protocols [24], and by tests of Bell’s inequalities [25–29], which inherently require to discretize the homodyne outcomes to binary values.

Optical homodyne detectors are ubiquitous in telecommunications and can even be found on optical satellites already in orbit. Such satellites are promising candidates for exploring quantum technology and bringing fundamental tests of quantum mechanics to space both rapidly and cost-effectively. Satellite links, however, imply considerable channel loss which reduces the observable squeezing value. Moreover, as currently the primary application of optical satellites is classical communication via binary phase-shift keying, only the sign of the homodyne signal is relevant and the data is often projected into binary outcomes during signal processing [30, 31]. The question arises whether under such strong technical constraints quadrature squeezing can still be detected.

Extreme discretization into binary outcomes has been studied extensively for photon number measurements. Photon “on-off” detection and the photon number parity measurement were shown to allow for (near-) optimal applications in quantum state discrimination [32–36] and quantum optical metrology [37–42]. Discretized

homodyne detection schemes were used for witnessing single photon entanglement [43] and for super-resolved imaging with coherent states [44].

In this Letter, we investigate fundamental limits of discretized homodyne measurements, particularly focusing on the detection of quadrature squeezing. We consider the extreme case of a binary homodyne detector (BHD) that simply distinguishes between positive and negative quadrature values and we analyze its performance for the detection of individual signals as well as for the consecutive detection of multiple copies of the same state. We show that despite the extreme constraint BHD can detect quadrature squeezing efficiently even under unfavorable conditions like high loss, when relying on ensemble measurements. The ratio between the required number of copies to obtain the same information about the observed signal - measured in terms of the Bayesian *a posteriori* probability - is merely 3.3 and is independent on the squeezing parameter. We complement our theoretical analysis with an experimental verification. To this end, we prepare and detect both a coherent state and a weakly squeezed state via BHD detection and compare the results to ideal, i.e. non-discretized, homodyne detection. We finally discuss the feasibility of detecting squeezed states via BHD detection in satellite links.

Binary Homodyne Detection– In the following, we introduce the binary homodyne observable and describe how its expectation value can be controlled via a coherent displacement. We consider detecting a Gaussian state, for which the ellipticity [23], i.e. the ratio between the major- and minor semi-axis of its phase space distribution, is unknown but has one of two possible values. The described detection scheme is insusceptible to whether the state is pure or mixed such that we can assume pure states. Moreover, the overlap between any two states remains unchanged when applying the same squeezing operation to both. We therefore assume that one state is a coherent state (the most classical state as expected under the influence of high loss) and the

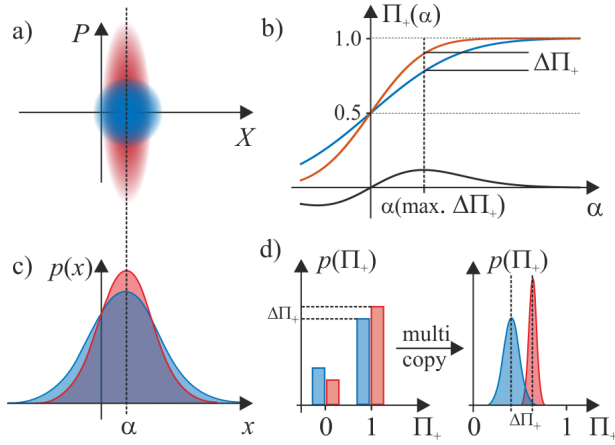


FIG. 1. a) Illustration of a coherent (blue) and a displaced squeezed vacuum state (red) in phase space. b) Binary homodyne expectation value Π_+ of the displaced states and their difference $\Delta\Pi_+(\alpha)$ (black) as a function of the displacement amplitude α . c) Ideal homodyne marginal distributions along the squeezed x -quadrature. d) Sketch of the statistical BHD probability distribution $p(\Pi_+)$ obtained via single-copy and a multi-copy detection.

other state is a squeezed state with the same mean amplitude and with a real-valued squeezing parameter r (see Fig. 1(a)).

To identify the received signal via a BHD, the signal is first displaced in phase space, followed by a projection onto quadrature semi-axes. This measurement is described by two positive operator-valued measure elements (POVM)

$$\begin{aligned}\hat{\Pi}_+(\alpha) &= \int_0^\infty dx \hat{D}^\dagger(\alpha)|x\rangle\langle x|\hat{D}(\alpha), \\ \hat{\Pi}_-(\alpha) &= I - \hat{\Pi}_+(\alpha),\end{aligned}\quad (1)$$

where α is the displacement amplitude. Owing to the symmetry along the quadrature axis, we can restrict the analysis to real and positive displacement amplitudes.

Decision Rule.—The BHD outcome is a Bernoulli random variable $Y(\alpha)$ over the sample space $y \in \{+, -\}$. The likelihood functions for the two hypotheses $\hat{\rho}_h \in \{\text{coh}, \text{sqz}\}$ are the conditional probabilities $P_{Y|H}(y|h) = \text{Tr}[\hat{\Pi}_y \hat{\rho}_h]$.

$$\begin{aligned}P_{Y|H}\left(\begin{matrix} + \\ - \end{matrix} \middle| \text{coh}, \alpha\right) &= \frac{1}{2} \left(1 \pm \text{erf}\left(\frac{\alpha}{\sqrt{2}}\right)\right), \\ P_{Y|H}\left(\begin{matrix} + \\ - \end{matrix} \middle| \text{sqz}, \alpha, r\right) &= \frac{1}{2} \left(1 \pm \text{erf}\left(\frac{\alpha}{\sqrt{2}e^{-2r}}\right)\right).\end{aligned}\quad (2)$$

The average *a posteriori* probability is derived by updating the priors ($P_H(\text{coh}) = P_H(\text{sqz}) = 1/2$) via Bayesian inference

$$\langle P_{H|Y}(\alpha, r) \rangle = \sum_{y=\{+,-\}} \frac{\sum_h P_{Y|H}(y|h, \alpha, r)^2}{2P_Y(y)}, \quad (3)$$

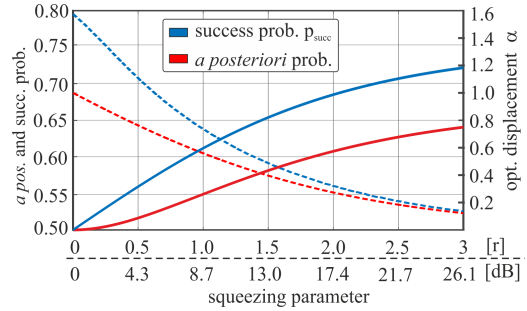


FIG. 2. Average *a posteriori* (red) and success probability (blue) for the detection of a single state, as well as the associated optimized displacement amplitudes α (dashed lines and right axis labels).

where $P_Y(y) = (P_{Y|H}(y|\text{coh}) + P_{Y|H}(y|\text{sqz}))/2$, and is optimized over the displacement α .

For positive α , $P_{Y|H}(+|\text{sqz}) > P_{Y|H}(+|\text{coh})$, such that the squeezed state can be associated with the outcome '+' and the coherent state with the outcome '-'. Fig. 1(b) shows the BHD expectation value $\langle \Pi_+(\alpha) \rangle$. Varying the displacement amplitude allows maximizing the difference $\Delta\Pi_+ = P_{Y|H}(+|\text{sqz}) - P_{Y|H}(+|\text{coh})$ between the expectation values and consequently allows for an optimized discrimination. The maximal success probability for a single detection is

$$p_{\text{succ}} = \max_{\alpha} \frac{1 + \Pi_+(\alpha)}{2} \quad (4)$$

The achievable success- and *a posteriori* probability, as well as the associated optimized displacement amplitudes are shown in Fig. 2 as a function of the squeezing parameter. Note, that the displacement amplitudes optimizing the two parameters coincide only in the limit of large squeezing amplitudes. This emphasizes that *a posteriori*- and success probability and are indeed distinct figures of merit. The *a posteriori* probability is maximized by optimizing the difference between the conditional probabilities for any possible outcome, while the optimal success probability requires maximizing $\Delta\Pi_+$. The optimal displacement in the latter case coincides with the intersection point of the states' marginal distributions as depicted in Fig. 1(c).

$$\alpha^{(\text{opt})}(r) = \sqrt{\frac{2r}{e^{2r} - 1}}. \quad (5)$$

In the limit of an infinitely squeezed state the optimized displacement asymptotically approaches zero $\lim_{r \rightarrow \infty} \alpha(r) = 0$, but the success probability is upper bounded by $p_{\text{succ}} \leq \frac{3}{4}$, as at least half of the coherent state has support on the positive semi-axis. Similarly, the *a posteriori* probability is upper bounded by $\langle P_{H|Y}(\alpha, r) \rangle \leq \frac{2}{3}$.

Multi-Copy Detection— To verify the properties of the quantum states after propagation it is sufficient to per-

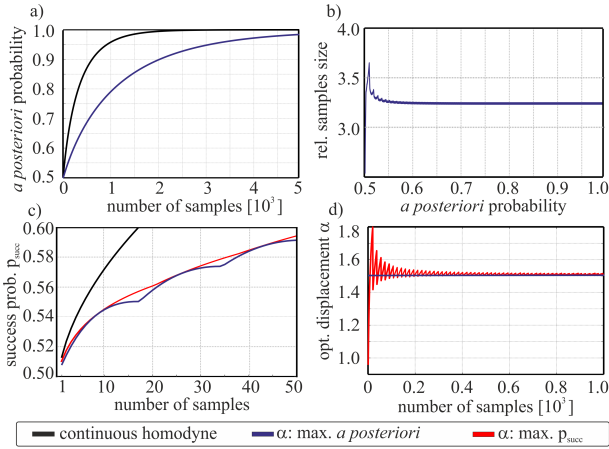


FIG. 3. a) *A posteriori* probabilities for non-discretized homodyne detection (black), and BHD detection as a function of the number of samples. The displacement is optimized for maximizing the *a posteriori* probability. b) Relative sample overhead required to obtain the same *a posteriori* probability for the BHD measurement as obtained by non-discretized homodyne detection. c) Probability for successful state discrimination as a function of the number of samples and for different displacement strategies. d) Comparison of the optimized displacement amplitudes α for different strategies.

form ensemble measurements. Gathering statistics over multiple measurements of identically prepared states allows reducing the overlap of the signals probability distributions (see Fig. 1(d)) and consequently reducing the error probability. Let $\vec{y} = (y_1, y_2, \dots, y_N)$ denote the outcome of a multi-copy BHD measurement.

The probability to detect $k \in \{0, 1, \dots, N\}$, positive quadrature projections from N measurements is given by the Binomial probability density function

$$P_{Y|H}^{(N)}(k|h, \alpha, r) = \binom{N}{k} P_{Y|H}(+|h, \alpha, r)^k (1 - P_{Y|H}(+|h, \alpha, r))^{N-k} \quad (6)$$

which approaches a quasi-continuous Gaussian distribution for a large number of samples.

The *a posteriori* probability for the signal hypothesis $h \in \{\text{coh}, \text{sqz}\}$ follows from the conditional single-copy probabilities in Eq.(2) and Eq.(3) via Bayesian inference as

$$P_{H|\vec{Y}}^{(N)}(h|\vec{y}) = \frac{\prod_{i=1}^N P_{Y|H}(y_i|h)}{\sum_h \prod_{j=1}^N P_{Y|H}(y_j|h)}. \quad (7)$$

The maximal *a posteriori* probability is obtained by maximizing over the displacement parameter α and is given by

$$\langle P_{H|\vec{Y}}^{(N)} \rangle = \max_{\alpha} \sum_{k=0}^N \frac{\sum_h [P_{Y|H}^{(N)}(k|h, \alpha, r)]^2}{2 \sum_{h'} P_{Y|H}^{(N)}(k|h', \alpha, r)}. \quad (8)$$

This quantity is compared to a non-discretized homodyne detector in Fig. 3(a) for the example of a squeez-

ing parameter $r = 0.085$, i.e. 0.369 dB below the shot noise level. Naturally, the outcomes of the BHD yield less information about the detected states than ideal homodyne detection. (For details on the calculation of the *a posteriori*- and success probability for ideal homodyne detection see Supplemental Material A.) Consequently, a larger number of samples has to be collected on average to achieve the same *a posteriori* probability. The required relative sample size is depicted in Fig. 3(b). Apart from the region of *a posteriori* probabilities close to 0.5, where statistical effects originating from the discreteness of the Binomial distribution are most pronounced, the ratio is essentially constant and has a value of merely 3.3. A separate analysis shows that this ratio is independent of the squeezing parameter r . We stress that this value, as it applies to the extreme discretization into binary outcomes, is indeed an upper bound for the required sample overhead of arbitrarily discretized homodyne detection as e.g. occurring in realistic analog-to-digital (AD) converters.

The optimal success probability p_{succ} in multi-copy detection is obtained by generalizing Eq.(4) such that the squeezed state is hypothesized whenever k equals or exceeds a threshold value τ , followed by maximizing over τ and α .

$$P_{succ}^{(N)}(k) = \max_{\alpha, \tau} \frac{P^{(N)}(k \leq \tau | \text{coh}, \alpha) + P^{(N)}(k > \tau | \text{sqz}, \alpha, r)}{2} \quad (9)$$

Fig. 3(c) compares the optimized success probability of the BHD to an ideal homodyne detector as well as to a BHD where the displacement maximizing the *a posteriori* probability was applied. Maximizing the *a posteriori* probability is only equivalent to minimizing the error probability in the limit of a large number of samples. This is underpinned by Fig. 3(d) where the distinct optimized displacements are illustrated. The fluctuations in the displacement maximizing the success probability originate from the discreteness of the underlying Binomial distribution. A more detailed discussion is given in Supplemental Material Sec. B.

Experimental Validation.— We experimentally prepared a vacuum state and a weakly squeezed vacuum state ($r = 0.085$; 0.369 dB) using the fiber-based polarization squeezing setup [45] outlined in Fig. 4(a). Pulses from a shot-noise limited laser centered at 1560 nm are distributed equally on the principal axes of a 13 m long polarization maintaining fiber and get individually squeezed via the Kerr nonlinearity [46]. The emerging pulses are locked to circular polarization such that the mean value of the squeezed polarization state lies along the S_3 direction on the Poincaré sphere. Homodyne detection of the quantum Stokes variables within the *dark* $S_1 - S_2$ plane is then equivalent to conventional homodyne detection in the canonical $x-p$ phase space. A detailed description of the setup and the theoretical background can be found in [47]. In total, we

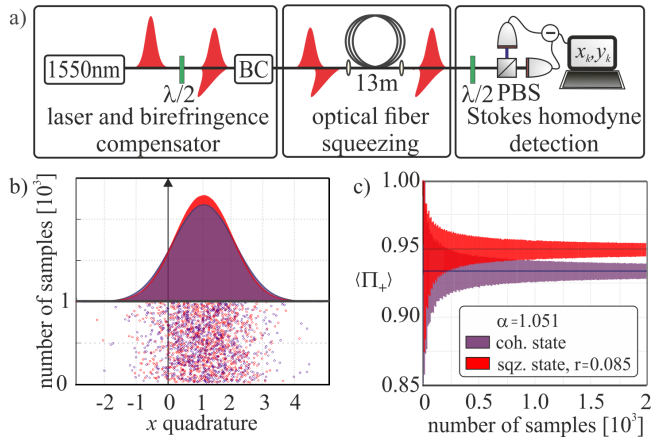


FIG. 4. a) Outline of the experimental setup. b) Measured marginal distributions of the coherent state (purple) and of the squeezed state (red) with $r = 0.085$; i.e. 0.369 dB. An excerpt of displaced homodyne samples for both states is displayed in the lower section. c) Statistical distribution of the quadrature-parity observable as a function of the observed number of samples. The solid lines indicate the average quadrature-parity.

acquired $2 \cdot 10^8$ homodyne samples $\{x_k\}$ of identically prepared copies of the vacuum and the squeezed state projected along the squeezed quadrature. The detector resolution is 16 bit, such that the quadrature was sampled quasi-continuously and the data provides accurate histograms of the actual marginal distribution as shown in Fig. 4(b). Applying a coherent displacement solely adds a *classical* offset amplitude to the quantum field operator, $\hat{a} \mapsto \hat{a} + \alpha$, and consequently to the detected quadrature, $\hat{X} \mapsto \hat{X} + \text{Re}(\alpha)$, where $\hat{X} = (\hat{a} + \hat{a}^\dagger)/2$. Therefore, given the quasi-continuous homodyne samples $\{x_k\}$, the coherent displacement and the subsequent projection onto the quadrature semi-axes $y_k \in \{+, -\}$ can faithfully be performed after detection via $x_k \mapsto y_k = \frac{1}{2} (\text{sign}(x_k + \alpha) + 1)$.

The statistical distribution of the BHD samples for the measured coherent (purple) and squeezed state (red) are shown in Fig. 4(c) for a displacement amplitude $\alpha = 1.501$ which maximizes the *a posteriori* probability. The distributions are largely overlapping for a small number of samples, but eventually become distinguishable with increasing sample size.

Fig. 5 shows the experimentally obtained statistical distribution of the *a posteriori* probabilities for BHD detection as a function of the number of samples. The discreteness of the sample distributions yields a rich structure which is consistent with numerical simulations. For a large number of samples the *a posteriori* probability converges to unity as could be expected. The dashed white curve shows the average *a posteriori* probability which also is in excellent agreement with theoretical predictions.

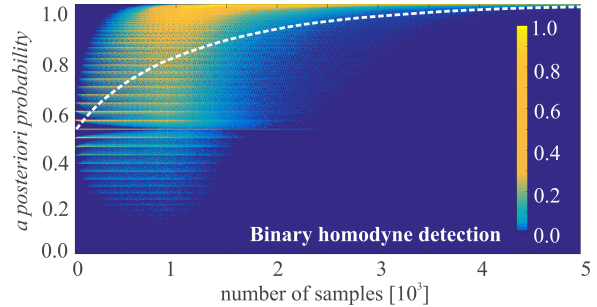


FIG. 5. Statistical distributions of the experimentally obtained *a posteriori* probabilities as a function of the number of detected samples N . For improved contrast, the maximal *a posteriori* probability for each value of N has been normalized to unity. The dashed white curve shows the average value for each number of detections.

Observing Squeezing in Optical Satellite Links.— Optical communication satellites are currently optimized for the detection of binary encoded classical signals. This encompasses projecting the signals into binary outcomes already in the detection process, which thus prevents an evaluation of the continuous-variable quantum information. Our results on BHD detection pave the way to nevertheless detect quadrature squeezing in such scenarios. Let us investigate how the size of the measurement data required to faithfully detect a squeezed state scales as a function of loss in the transmission channel (see Supplemental Material C for details). An up-link from a ground-based sender to a low Earth orbit (LEO) satellite receiver (≈ 600 km distance) with transmitter and receiver apertures of about 30 cm diameter is subject to transmission losses of about 40–45 dB [48]. These losses includes atmospheric turbulence, diffraction and pointing error. Let us further assume a moderate squeezing parameter of $r = 0.69$, corresponding to 6 dB of squeezing below the shot noise level, and let us bound the average error probability to at most 10^{-2} . To satisfy this realistic scenario for 40 dB of loss, about $3 \cdot 10^9$ BHD samples are required, while 45 dB of loss would require $3 \cdot 10^{10}$ samples. We stress again that this is of the same order of magnitude as the number of samples required by a non-discretized homodyne detector, differing merely by a constant factor of 3.3. Optical homodyne detection and quadrature squeezing have been demonstrated with GHz bandwidths [49, 50], such that the acquisition of the required number of samples can be achieved within a few seconds, i.e. well within the typical link time for a single flyover of a LEO satellite (≈ 300 seconds). We thus emphasize that it is, in principle, feasible with technology already in orbit to detect squeezing in optical satellite links.

Conclusions.— Homodyne detection is a powerful quantum measurement even under the constraint of severe

discretization. Our work underlines this by showing that a homodyne detector with a resolution of only one bit can still accomplish the quintessential task of detecting squeezed light efficiently. We derived the optimal phase space displacements for maximizing the success probability and the *a posteriori* probability, and found that a binary homodyne detector can distinguish two Gaussian states of different squeezing parameter with the same *a posteriori* probabilities as its non-discretized counterpart by detecting a sample set merely a factor of 3.3 larger. Our work opens prospects for detecting quantum squeezing in optical satellite links. A possible early experimental demonstration might involve using (binary) homodyne detection on the satellite and an Earth-to-satellite communication link with a squeezer at the ground station, that includes the necessary techniques for phase front precompensation and phase locking.

We thank Gerd Leuchs, Ulrik L. Andersen and Dominique Elser for fruitful discussions.

-
- [1] P. Shadbolt, J. C. F. Mathews, A. Laing, and J. L. O’Brien, *Nature Physics* **10**, 278 (2014).
- [2] J. G. Rarity, P. R. Tapster, P. M. Gorman, and P. Knight, *New Journal of Physics* **4**, 82 (2002).
- [3] Ursin, R., Jennewein, T., Kofler, J., Perdigue, J. M., Cacciapuoti, L., de Matos, C. J., Aspelmeyer, M., Valencia, A., Scheidl, T., Acin, A., Barbieri, C., Bianco, G., Brukner, C., Capmany, J., Cova, S., Giggenbach, D., Leeb, W., Hadfield, R. H., Laflamme, R., Lütkenhaus, N., Milburn, G., Peev, M., Ralph, T., Rarity, J., Renner, R., Samain, E., Solomos, N., Tittel, W., Torres, J. P., Toyoshima, M., Ortigosa-Blanch, A., Pruneri, V., Villoresi, P., Walmsley, I., Weihs, G., Weinfurter, H., Zukowski, M., and Zeilinger, A., *Europhysics News* **40**, 26 (2009).
- [4] Z. Merali, *Nature* **492**, 22 (2012).
- [5] K. Günthner, I. Khan, D. Elser, B. Stiller, O. Bayraktar, C. R. Müller, K. Sauke, D. Tröndle, F. Heine, S. Seel, P. Greulich, H. Zech, B. Gütllich, S. Philipp-May, C. Marquardt, and G. Leuchs, *Optica* **4**, 611 (2017).
- [6] F. Vedovato, C. Agnesi, M. Schiavon, D. Dequal, L. Calderaro, M. Tomasin, D. Giacomo Marangon, A. Stanco, V. Luceri, G. Bianco, G. Vallone, and P. Villoresi, *Sci. Adv.* **3** (2017), <https://doi.org/10.1126/sciadv.1701180>.
- [7] D. Rideout, T. Jennewein, G. Amelino-Camelia, T. F. Demarie, B. L. Higgins, A. Kempf, A. Kent, R. Laflamme, X. Ma, R. B. Mann, E. Martin-Martinez, N. C. Menicucci, J. Moffat, C. Simon, R. Sorkin, L. Smolin, and D. R. Terno, *Classical and Quantum Gravity* **29**, 224011 (2012).
- [8] C. Weedbrook, S. Pirandola, R. García-Patrón, N. J. Cerf, T. C. Ralph, J. H. Shapiro, and S. Lloyd, *Rev. Mod. Phys.* **84**, 621 (2012).
- [9] U. L. Andersen, T. Gehring, C. Marquardt, and G. Leuchs, *Physica Scripta* **91**, 053001 (2016).
- [10] H. P. Yuen and V. W. S. Chan, *Optics Letters* **8**, 177 (1983).
- [11] M. Aspelmeyer, T. J. Kippenberg, and F. Marquardt, *Rev. Mod. Phys.* **86**, 1391 (2014).
- [12] A. A. Houck, D. I. Schuster, G. J. M., J. A. Schreier, B. R. Johnson, C. J. M., L. Frunzio, J. Majer, M. H. Devoret, S. M. Girvin, and S. R. J., *Nature* **449**, 328 (2007).
- [13] S. Filipp, P. Maurer, P. J. Leek, M. Baur, R. Bianchetti, J. M. Fink, M. Göppl, L. Steffen, J. M. Gambetta, A. Blais, and A. Wallraff, *Phys. Rev. Lett.* **102**, 200402 (2009).
- [14] A. Kuzmich and E. S. Polzik, in *Quantum Information with Continuous Variables* (Springer, 2003) pp. 231–265.
- [15] N. J. Cerf, G. Leuchs, and E. S. Polzik, *Quantum information with continuous variables of atoms and light* (Imperial College Press, 2007).
- [16] R. Namiki, S. I. R. Tanaka, T. Takano, and Y. Takahashi, *Applied Physics B* **105**, 197 (2011).
- [17] C. R. Müller, L. S. Madsen, A. B. Klimov, L. L. Sánchez-Soto, G. Leuchs, C. Marquardt, and U. L. Andersen, *Phys. Rev. A* **93**, 033816 (2016).
- [18] J. Estève, C. Gross, A. Weller, S. Giovanazzi, and O. M. K., *Nature* **455**, 1216 (2008).
- [19] S. L. Braunstein and P. van Loock, *Rev. Mod. Phys.* **77**, 513 (2005).
- [20] D. T. Smithey, M. Beck, M. G. Raymer, and A. Faridani, *Phys. Rev. Lett.* **70**, 1244 (1993).
- [21] U. Leonhardt, *Measuring the quantum state of light*, Vol. 22 (Cambridge university press, 1997).
- [22] A. I. Lvovsky and M. G. Raymer, *Rev. Mod. Phys.* **81**, 299 (2009).
- [23] C. R. Müller, C. Peuntinger, T. Dirmeier, I. Khan, U. Vogl, C. Marquardt, G. Leuchs, L. L. Sánchez-Soto, Y. S. Teo, Z. Hradil, and J. Řeháček, *Phys. Rev. Lett.* **117**, 070801 (2016).
- [24] Y.-B. Zhao, M. Heid, J. Rigas, and N. Lütkenhaus, *Phys. Rev. A* **79**, 012307 (2009).
- [25] A. Gilchrist, P. Deuar, and M. D. Reid, *Phys. Rev. A* **60**, 4259 (1999).
- [26] W. J. Munro, *Phys. Rev. A* **59**, 4197 (1999).
- [27] G. Auberson, G. Mahoux, S. Roy, and V. Singh, *Physics Letters A* **300**, 327 (2002).
- [28] K. Banaszek and K. Wódkiewicz, *Phys. Rev. Lett.* **82**, 2009 (1999).
- [29] K. P. Seshadreesan, C. F. Wildfeuer, M. B. Kim, H. Lee, and J. P. Dowling, *Quantum Information Processing* **15**, 1025 (2016).
- [30] S. Schaefer, M. Gregory, and W. Rosenkranz, *Opt. Eng.* **55**(11), 111614 (2016).
- [31] F. Heine, G. Mühlwinkel, H. Zech, D. Tröndle, S. Seel, M. Motzigemba, R. Meyer, S. Philipp-May, and E. Benzi, *Proc. SPIE* **93540G** (2015), 10.1117/12.2083117.
- [32] S. J. Dolinar, *An optimum receiver for the binary coherent state quantum channel.*, Quarterly Progress Report 111: 115-120. (MIT Research Laboratory of Electronics, 1973).
- [33] C. Wittmann, M. Takeoka, K. N. Cassemiro, M. Sasaki, G. Leuchs, and U. L. Andersen, *Phys. Rev. Lett.* **101**, 210501 (2008).
- [34] M. Takeoka and M. Sasaki, *Phys. Rev. A* **78**, 022320 (2008).
- [35] C. Wittmann, U. L. Andersen, M. Takeoka, D. Sych, and G. Leuchs, *Phys. Rev. Lett.* **104**, 100505 (2010).
- [36] M. M. Wilde, S. Guha, S. H. Tan, and S. Lloyd, in *Information Theory Proceedings (ISIT), 2012 IEEE International Symposium on* (2012) pp. 551–555.
- [37] J. P. Dowling and K. P. Seshadreesan, *J. Lightwave Technol.* **33**, 2359 (2015).
- [38] R. Demkowicz-Dobrzański, M. Jarzyna, and J. Kołodyński, *Progress in Optics* **60**, 345 (2015).

- [39] K. P. Seshadreesan, S. Kim, J. P. Dowling, and H. Lee, *Phys. Rev. A* **87**, 043833 (2013).
- [40] K. P. Seshadreesan, P. M. Anisimov, H. Lee, and J. P. Dowling, *New Journal of Physics* **13**, 083026 (2011).
- [41] P. M. Anisimov, G. M. Raterman, A. Chiruvelli, W. N. Plick, S. D. Huver, H. Lee, and J. P. Dowling, *Phys. Rev. Lett.* **104**, 103602 (2010).
- [42] K. R. Motes, J. P. Olson, E. J. Rabeaux, J. P. Dowling, S. J. Olson, and P. P. Rohde, *Phys. Rev. Lett.* **114**, 170802 (2015).
- [43] O. Morin, J.-D. Bancal, M. Ho, P. Sekatski, V. D'Auria, N. Gisin, J. Laurat, and N. Sangouard, *Phys. Rev. Lett.* **110**, 130401 (2013).
- [44] E. Distanto, M. Ježek, and U. L. Andersen, *Phys. Rev. Lett.* **111**, 033603 (2013).
- [45] J. Heersink, V. Josse, G. Leuchs, and U. L. Andersen, *Opt. Lett.* **30**, 1192 (2005).
- [46] M. Kitagawa and Y. Yamamoto, *Phys. Rev. A* **34**, 3974 (1986).
- [47] C. R. Müller, B. Stoklasa, C. Peuntinger, C. Gabriel, J. Řeháček, Z. Hradil, A. B. Klimov, G. Leuchs, C. Marquardt, and L. L. Sánchez-Soto, *New Journal of Physics* **14**, 085002 (2012).
- [48] J.-P. Bourgoin, E. Meyer-Scott, B. L. Higgins, B. Helou, C. Erven, H. Hübel, B. Kumar, D. Hudson, I. D'Souza, R. Girard, R. Laflamme, and T. Jennewein, *New Journal of Physics* **15**, 023006 (2013).
- [49] C. Gabriel, C. Wittmann, B. Hacker, W. Mauerer, E. Huntington, M. Sabuncu, C. Marquardt, and G. Leuchs, in *Conference on Lasers and Electro-Optics 2012* (Optical Society of America, 2012) p. JW4A.103.
- [50] S. Ast, M. Mehmet, and R. Schnabel, *Opt. Express* **21**, 13572 (2013).

SUPPLEMENTAL MATERIAL

A. *A posteriori* probabilities for non-discretized homodyne detection

The *a posteriori* probability for ideal, i.e. non-discretized, homodyne detection is derived from the statistical distribution of the measured quadrature variance $\sigma_N^2 = \sum_{k=1}^N x_k^2/N$, where x_k are the continuous homodyne samples. The observed quadrature variance follows a χ_N^2 distribution, which is scaled such that the expectation value coincides with the mean quadrature variance of the detected state.

Given the observation of the quadrature variance σ_N^2 , the *a posteriori* probability for the hypothesis $h \in \{\text{coh}, \text{sqz}\}$ is

$$P_{H|Y}(h|\sigma_N^2) = \frac{P_{Y|H}(\sigma_N^2|h)}{P_{Y|H}(\sigma_N^2|\text{coh}) + P_{Y|H}(\sigma_N^2|\text{sqz})}, \quad (10)$$

The average *a posteriori* probability is obtained via integration over the scaled χ_N^2 probability distribution for observing the quadrature variance σ_N^2

$$\langle P_H \rangle = \frac{1}{2} \sum_h \int_0^\infty P_{Y|H}(\sigma_N^2|h) \cdot P_{H|Y}(h|\sigma_N^2) d\sigma_N^2 \quad (11)$$

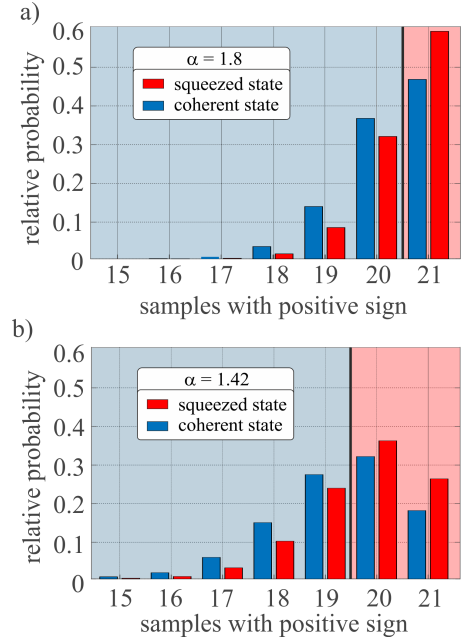


FIG. 6. Comparison of the statistical distributions for $N = 21$ samples and for different displacement amplitudes. a) $\alpha = 1.8$: opt. displacement just before the discontinuity at $N = 20$. a) $\alpha = 1.42$: opt. displacement just after the discontinuity at $N = 21$.

In the state discrimination scenario, the state with the higher *a posteriori* probability $\langle P_H(h) \rangle > 1/2$ is hypothesized.

$$\begin{aligned} H &= \text{sqz} \\ P_{H|Y}(\text{sqz}|\sigma_N^2) &\begin{matrix} > \\ < \end{matrix} P_{H|Y}(\text{coh}|\sigma_N^2). \quad (12) \\ H &= \text{coh} \end{aligned}$$

B. Discontinuous optimal displacement amplitude in maximizing the success probability

The Binomial probability density functions (see Eq.(6)) for the projection of 21 copies of the coherent state and the squeezed state onto the positive quadrature semi-axis Π_+ are shown for different displacement amplitudes α in Fig. 6. The blue-shaded areas indicates the cumulative quadrature-parity outcomes that lead to the hypothesis for the coherent state while outcomes in the red-shaded area are identified as the squeezed state. The distribution in Fig. 3(a) is obtained with the displacement amplitude maximizing the success probability for $N = 20$ copies, $\alpha = 1.8$, i.e. just before the discontinuity. In this configuration, the measurement hypothesizes the squeezed state only if all ($k = 21$) detected states are projected onto a positive quadrature value. Fig. 3(b) shows the distribution at the actual optimal displacement amplitude $\alpha = 1.42$. The state

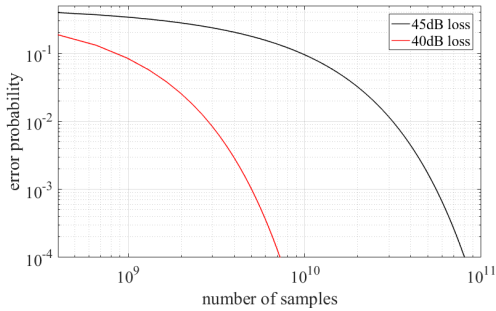


FIG. 7. Average minimum error probability as a function of the number of measured samples for the detection of a beam of light initially squeezed 6 dB below the shot noise level at the output of a lossy channel of (a) 40 dB loss, and (b) 45 dB loss.

is identified as the squeezed state if $k = 20$ or $k = 21$ detections had a positive quadrature projection. The discontinuities in the optimized displacement curve result from discrete shifts in the decision threshold com-

bined with the maximization of the likelihoods of the coherent and squeezed state distributions on their respective identification domains. For a large number of copies N the range of possible outcomes approaches a quasi-continuous Gaussian distribution and the optimized displacement approaches an asymptotically optimal value.

C. Required samples size for squeezing detection in LEO satellite links

Fig. 7 depicts the error probability for the unbiased detection of squeezed states (6 dB, $r = 0.69$) emerging from a lossy channel of 40 dB and 45 dB. On an absolute scale, the error probability remains nearly constant up to a certain number of detected samples, but thereafter drops steeply with increasing number of samples. The plot shows that squeezing can be detected with an average error probability no greater than 10^{-2} by measuring $3 \cdot 10^9$ (40 dB) samples and $3 \cdot 10^{10}$ (45 dB) samples, respectively.